Characterization of the Transverse Coherence of Hard Synchrotron Radiation by Intensity Interferometry

M. Yabashi,[1] K. Tamasaku,[2] and T. Ishikawa[1,2]
[1]*SPring-8/JASRI, Mikazuki, Hyogo 679-5198, Japan*
[2]*SPring-8/RIKEN, Mikazuki, Hyogo 679-5148, Japan*
(Received 20 June 2001; published 14 September 2001)

The transverse coherence of x rays was measured with an intensity interferometer using a 120-μeV-bandwidth monochromator operating at 14.41 keV. By analyzing the transverse coherence profiles, a vertical source profile of a 25-m long undulator of SPring-8, as well as the coherence degradation by a phase object in the beam path, were quantitatively characterized.

DOI: 10.1103/PhysRevLett.87.140801 PACS numbers: 07.85.Qe, 41.50.+h, 42.50.−p

In the hard x-ray region, quantitative characterization of the transverse coherence [1] is important for giving a basis for coherent x-ray optics such as phase-contrast imaging and in-line holography [2–6]. Propagation of the transverse coherence through various optical components including crystals, mirrors, windows, and filters should be investigated for full utilization of coherent x rays. Furthermore, one can determine a transverse source profile in vertical, which is of the order of 10 μm, at the third generation synchrotron facilities by characterizing the transverse coherence. This leads to evaluation of the straightness of the electron trajectory along an undulator, which is important for realizing a free electron laser (FEL) based on self-amplified spontaneous emission (SASE) toward a shorter wavelength (down to 1 Å) operation.

The x-ray transverse coherence at the third generation synchrotron facilities have been evaluated through applications such as nuclear forward scattering [7] and in-line holography [6]. More directly, the transverse coherence is measured by the wave-front dividing interferometry [1]. Although such x-ray interferometers using perfect crystal are being developed [8,9], they have not been applied to general conditions yet.

Intensity interferometry is another straightforward method to characterize the transverse coherence [10]. For the chaotic light, the second-order degree of coherence, $\gamma^{(2)}$, has a value between 1 ($M = \infty$, incoherent) and 2 ($M = 1$, coherent), where M is the number of the optical modes within a three-dimensional (two transverse and one longitudinal) beam volume [11]. One can consequently characterize the transverse coherence only by changing an aperture size for detectors. This simple scheme facilitates the optical design of the interferometer. Furthermore, intensity interferometry using a fast coincidence technique is applicable even for the instable optics, where the amplitude interference would be smeared out.

To observe intensity interference between high-energy photons from synchrotron radiation using the coincidence technique, the following two points are essential [12]. One is the extension of the longitudinal coherence length s_t, which should not be negligibly smaller than the electron bunch length σ_t (typically a few millimeters), by using a high-resolution monochromator (HRM). This assures a higher value of $\gamma^{(2)}$. The other is the high brilliance of light source, which decreases the statistical error of the coincidence counting. Undulator radiation is desirable as high brilliant source in the short wavelength region. So far, several intensity interferometers for undulator radiation have been developed in the soft x-ray region [13,14], as well as the hard x-ray region [15,16]. The chaotic photon statistics of the undulator radiation has been deduced from these experimental results. However, the maximum $\gamma^{(2)} - 1$ was still 0.010 ± 0.002 ($M = 100$) even using a HRM with a 5.5 meV bandwidth at 14.41 keV [16]. The statistical counting errors have limited accuracy for further analysis. Moreover, the HRMs employed there might change or degrade the transverse coherence in vertical direction, because of imperfect surface finish, the use of asymmetric reflections, and limited acceptances.

In this Letter, we present direct and quantitative characterization of the x-ray transverse coherence in vertical direction using a new x-ray intensity interferometer. The interferometer consists of a state-of-the-art high-resolution monochromator, which has a 120 μeV bandwidth at 14.41 keV [17], a precision four-jaw slit, two semitransparent detectors and coincidence circuits. The x-ray transverse coherence was characterized under different conditions. The vertical source profile of an undulator, as well as the coherence degradation by a phase object in the beam path, are quantitatively discussed.

We assume that the spatial profiles of the light source are represented as Gaussian distributions with widths (1σ) of s_x and s_y in horizontal and vertical directions, respectively, and the temporal profile (bunch structure) also as a Gaussian with a bunch length (1σ) of s_t. A rectangular slit ($w_x \times w_y$ in full widths) is placed at a distance L from the source. The transverse coherence lengths, σ_x and σ_y (for horizontal and vertical, respectively), at the slit position are given by

$$\sigma_i = \frac{\lambda L}{2\pi s_i}, \qquad (i = x, y). \tag{1}$$

A high-resolution monochromator selects a Gaussian energy spectrum with a bandwidth of ΔE in full width at half

maximum (FWHM) from the incident radiation at a central energy of E (wavelength of λ). The longitudinal coherence length σ_t is written as $\alpha\lambda^2/\Delta\lambda$, where $\Delta\lambda = \lambda\Delta E/E$ and $\alpha = [(\ln 2)/2]^{1/2}/\pi$.

Using two detectors and a coincidence circuit, we measure the coincidence counting C_S between signals from the same bunch, as well as the accidental coincidence C_N. Then the second-order degree of coherence $\gamma^{(2)}$ for the polarized chaotic light is represented by using the numbers of the optical modes along a longitudinal (M_t) and two transverse (M_x and M_y for horizontal and vertical, respectively) directions as [11,12]

$$\gamma^{(2)} = C_S/C_N = 1 + M_t^{-1}M_x^{-1}M_y^{-1}, \tag{2}$$

where $M_t^{-1} = \sigma_t/(\sigma_t^2 + s_t^2)^{1/2}$, and

$$M_i^{-1} = M_{\mathrm{Gauss}}^{-1}(w_i, \sigma_i) = \frac{\sqrt{\pi}\,\sigma_i}{w_i}\,\mathrm{erf}\left(\frac{w_i}{\sigma_i}\right) - \frac{\sigma_i^2}{w_i^2}\left[1 - \exp\left(\frac{w_i^2}{\sigma_i^2}\right)\right], \quad (i = x, y). \tag{3}$$

One can characterize the transverse coherence profile $M_y^{-1}(M_x^{-1})$ by changing the slit width $w_y^{-1}(w_x^{-1})$ with keeping the other conditions constant.

The experiment was performed at a beam line 19LXU [18] for a 25-m long undulator of SPring-8 [19] (Fig. 1). A filling pattern of the storage ring at the experiment was a 175-bunch mode (minimum bunch interval of 23.6 nsec) with a maximum total current of 100 mA. A cryogenically cooled Si 111 double-crystal monochromator (DCM) selected 14.41 keV radiation, which was the first harmonic of the undulator radiation at an undulator gap of 20.3 mm. As other objects in the beam path, we have two 0.25-mm-thick

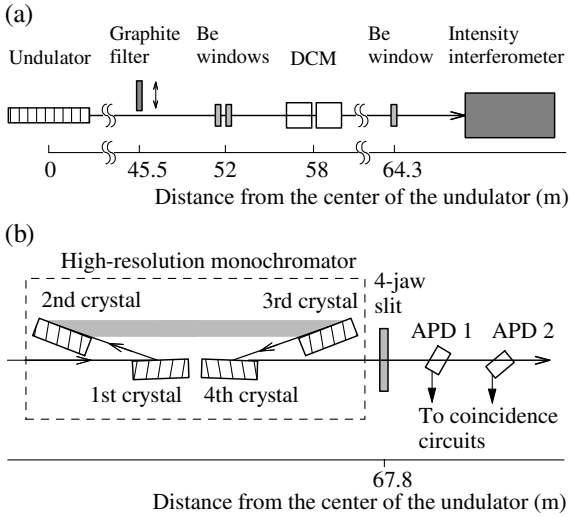

FIG. 1. Schematic top view of the experimental setup (a), and that of the intensity interferometer (b). The interferometer consists of a high-resolution monochromator using four separated crystals, a precision four-jaw slit, two semitransparent avalanche photodiodes (APDs), and coincidence circuits.

Be windows in a front-end section, and one 0.2-mm-thick Be window at the end of the transport channel. The Be windows were well polished (surface roughness of less than 1 μm rms) to avoid coherence degradation. A 0.9-mm-thick graphite filter in the front end is optionally inserted into the beam path in order to decrease a thermal load on the first Be window [20], while it can be retracted at a present heat-load condition. The graphite filter is regarded as a phase object that degrades the coherence because of its large density fluctuation.

The intensity interferometer was composed by using a high precision diffractometer installed in an end station [18]. An HRM with in-line geometry, where the exit beam goes parallel to the incidence, was employed in order to extend the longitudinal coherence length. The combination of four Si 11 5 3 reflections (Bragg angles of 80.4°) with highly asymmetric reflections (asymmetric factors $b_1 = b_2 = 1/b_3 = 1/b_4 = 1/10.4$) realized an extremely narrow bandwidth $\Delta E = 120$ μeV at 14.41 keV ($\Delta E/E = 8 \times 10^{-9}$) [17]. The longitudinal coherence length $\sigma_t = 1.94$ mm was comparable to the bunch length $s_t = 5$ mm of the SPring-8 storage ring [21]. To preserve the transverse coherence through the HRM, there are several crucial problems to be addressed. One is to realize good surfaces for the HRM crystals, especially because they are employed in the grazing incidence conditions. With a conventional HRM using channel-cut crystals [7,15,16,22], the complicated crystal design has prevented ones from fabricating a fine surface finish. In contrast, our HRM design constituting of the four flat crystals allowed us to make high-quality surfaces by mechanochemical polishing. Another problem is that the crystal geometry using four-bounced asymmetric reflections introduces considerable complications into analysis, because each asymmetric reflection changes the transverse coherence in the scattering plane [9,23]. However, one may avoid such change of the coherence in the direction perpendicular to the scattering plane. To preserve the coherence in the vertical direction, we operated the HRM with the horizontal diffractions. This geometry consequently allowed us to avoid limiting the HRM acceptances in vertical, while the acceptances in the horizontal direction were restricted within 6.5 μrad (FWHM) in angle and 0.1 mm in space.

To adjust a beam size for detectors, a stepper-motor-driven four-jaw slit (step size of 0.25 μm for each blade) was placed at the exit of the HRM. The distance L from the light source (the center of the undulator) to the slit was 67.8 m. For the coincidence measurement, we arranged two semitransparent avalanche photo diodes (each diameter and thickness of 3 mm and 135 μm, respectively) in tandem. The inclination angles of the diodes to the beam axis were independently adjusted in order to increase detector efficiencies and to balance the counting rates between them. Finally, each detector counted 1/3 of the photons emerging from the slit. The coincidence counting C_S between signals originating from the same bunch

was measured using a coincidence circuit with a resolving time of around 3 nsec. Since this value was smaller than the minimum bunch separation, the effective time resolution of the coincidence system was reduced to the electron bunch width of 40 ps (FWHM) [12]. The accidental coincidence C_N was measured as the coincidence between signals with an interval of one revolution in the storage ring (4.79 μs), similar to the method described in Ref. [15].

Figure 2 shows measured $\gamma^{(2)} = C_S/C_N$ as a function of the vertical slit width. A horizontal slit width was fixed at 10 μm ($M_x = 1.1$) [24]. The graphite filter was not used in this measurement. The maximum $\gamma^{(2)} - 1$ reached 0.284 ± 0.015, which corresponds to the number of the optical modes $M = 3.52$. The total measurement time was 4 hours. On the contrary, measurements without the HRM ($M \sim 10^5$) gave $\gamma^{(2)} - 1 = 0.000\,89 \pm 0.0009$. This implies that we can neglect unwanted intensity fluctuation for the normalization, which may be induced by instability and/or decrease of the charge of the electron beam, during the delay time of 4.79 μs.

To characterize the transverse coherence through the function M_y^{-1}, the data were fitted based on Eqs. (2) and (3), as shown in Fig. 3(a). The agreement between the data and the fit shows a validity of the assumption that the source profile is Gaussian. The resulting coherence length $\sigma_y = 72.6$ μm corresponds to the apparent transverse source size $s_y = 12.8$ μm by Eq. (1). Although this value involves not only the true electron beam size but an additional term originating from the finite divergences of the electron and the photon beams [25], a contribution of the latter term to the apparent size is still small (within 10%) under this short wavelength condition. Therefore we regard the size s_y as a good approximation of the electron beam size. We compare the size to that obtained by an independent method. A visible light interferometer for bending magnet radiation [26] was simultaneously used for the purpose. The size deduced from the measurement with the visible light interferometer was converted to the electron beam size $s_{ref} = 15.9 \pm 1.5$ μm at the undulator section, using a design value of the betatron function of the storage ring. Small discrepancy between s_y and s_{ref} may originate from difference of the time resolutions of the detecting systems (40 ps and 1.7 ms for the intensity interferometer and visible light interferometer, respectively), because a drift of the source and/or the vibration of the optics can increase the apparent size in a longer integration time.

The interferometer was employed to study the coherence degradation by a phase object. The graphite filter was inserted into the beam path for the purpose. The measured results are shown in Fig. 3(b) as closed circles. We observed significant degradation of the transverse coherence. To explain the change of the coherence analytically, we assume that the source profile is represented by a sum of two independent Gaussians. Then the function M_y^{-1} is given by

$$M_y^{-1} = p^2 M_{\mathrm{Gauss}}^{-1}(w_y, \sigma_{1y}) + (1 - p)^2 M_{\mathrm{Gauss}}^{-1}(w_y, \sigma_{2y}) + 2p(1 - p) M_{\mathrm{Gauss}}^{-1}(w_y, \sigma_y^*), \quad (4)$$

where σ_{1y} and σ_{2y} are the coherence lengths originating from each Gaussian source, p is a ratio between the integrated intensities of two Gaussians, and $\sigma_y^* = \sigma_{1y}\sigma_{2y} \times [2/(\sigma_{1y}^2 + \sigma_{2y}^2)]^{1/2}$. The solid curve in Fig. 3(b) is a fit based on Eqs. (2) and (4) with fitting parameters $\sigma_{1y} = 75.7$ μm, $\sigma_{2y} = 6.2$ μm, $p = 0.498$, and $M_t^{-1} M_x^{-1} = 0.351$. The coherence length σ_{1y} was very close to σ_y given by the previous measurement. This indicates that the undulator source profile was extracted even when the

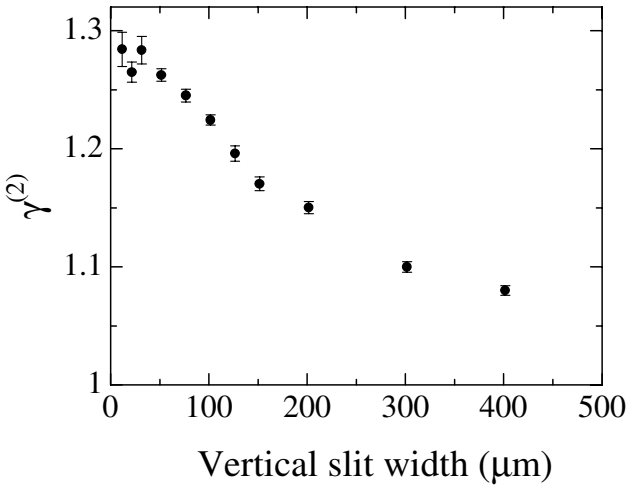

FIG. 2. The second-order degree of coherence $\gamma^{(2)} = C_S/C_N$, measured as a function of a vertical slit width w_y (without the front-end graphite filter). The error bars represent the statistical counting errors given by $(C_S^{-1} + C_N^{-1})^{1/2}$.

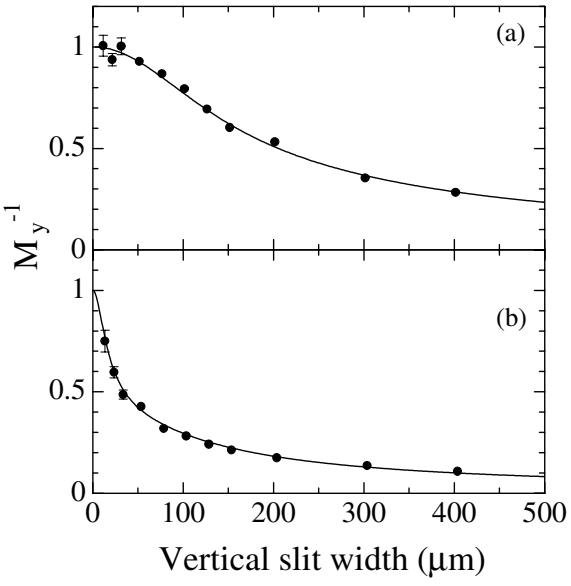

FIG. 3. The number of the optical modes M_y^{-1} as a function of a vertical slit width w_y without the graphite filter (a), and that with the graphite filter (b). The error bars represent the statistical counting errors given by $(C_S^{-1} + C_N^{-1})^{1/2}$. The solid lines are fits (see text).

source was partially screened by the phase object. The parameter p corresponds to the coherent fraction of the beam passing through the phase object. The coherence length σ_{2y} relates to the virtual source profile formed by the phase object. Assuming that the covariance of the refractive index of the phase object is a Gaussian distribution and neglecting the multiple interactions, we can estimate the correlation radius l_n of the phase object [3] to be around 10 μm.

In conclusion, we have developed an x-ray intensity interferometer using a 120-μeV-bandwidth monochromator at 14.41 keV. The vertical source profile of the 25-m long undulator was determined to be a Gaussian distribution with a width (1σ) of 12.8 μm, which corresponded to 0.19 μrad angular source size seen from the interferometer. The comparison of this value to an independent result given by visible light interferometry indicates the straightness of the electron trajectory along the 25-m long undulator. We note that the use of the hard x rays having a small emittance enabled us to diagnose such a small divergent source. Furthermore, we observed the coherence degradation by a phase object in the beam path. The measured coherence function was discriminated into two components, where one originated from the undulator source profile and the other from the virtual source caused by the phase object. Similar measurements will reveal the coherence propagation through various optical components in the x-ray region.

The authors thank Dr. H. Tanaka and Dr. M. Takao (SPring-8/JASRI) for the storage ring operation at the experiment, Dr. M. Masaki and Dr. S. Takano (SPring-8/JASRI) for the monitoring with the visible light interferometer, and Dr. S. Date and Dr. S. Kikuta (SPring-8/JASRI) for their fruitful discussions.

[1] M. Born and E. Wolf, *Principles of Optics* (Cambridge University Press, Cambridge, U.K., 1999), 7th ed.
[2] A. Snigirev, I. Snigireva, V. Kohn, S. Kuznetsov, and I. Schelokov, Rev. Sci. Instrum. **66**, 5486 (1995).
[3] R. Cloetens, R. Barrett, J. Baruchel, J. P. Guigay, and M. Schlenker, J. Phys. D **29**, 133 (1996).
[4] A. Momose and T. Takeda, Y. Itai, and K. Hirano, Nature Med. **2**, 473 (1996).
[5] Z. H. Hu, P. A. Thomas, A. Snigirev, I. Snigireva, A. Souvorov, P. G. R. Smith, G. W. Ross, and S. Teat, Nature (London) **392**, 690 (1998).
[6] V. Kohn, I. Snigireva, and A. Snigirev, Phys. Rev. Lett. **85**, 2745 (2000).
[7] A. Q. R. Baron, A. I. Chumakov, and H. F. Grünsteudel, H. Grünsteudel, L. Niesen, and R. Rüffer, Phys. Rev. Lett. **77**, 4808 (1996).
[8] U. Bonse and E. te Kaat, Z. Phys. **243**, 14 (1971).
[9] H. Yamazaki and T. Ishikawa, Proc. SPIE Int. Soc. Opt. Eng. **2856**, 279 (1996).
[10] R. Hanbury-Brown and R. Q. Twiss, Nature (London) **177**, 27 (1956).
[11] J. W. Goodman, *Statistical Optics* (Wiley, New York, 1985).
[12] E. Ikonen, Phys. Rev. Lett. **68**, 2759 (1992); E. Ikonen and R. Rüffer, Hyperfine Interact. **92**, 1089 (1994).
[13] E. Gluskin, I. McNulty, L. Yang, K. J. Randall, Z. Xu, and E. D. Johnson, Nucl. Instrum. Methods Phys. Res., Sect. A **347**, 177 (1994).
[14] R. Z. Tai, Y. Takayama, N. Takaya, T. Miyahara, S. Yamamoto, H. Sugiyama, J. Urakawa, H. Hayano, and M. Ando, Phys. Rev. A **60**, 3262 (1999).
[15] Y. Kunimune, Y. Yoda, K. Izumi, M. Yabashi, X. W. Zhang, T. Harami, M. Ando, and S. Kikuta, J. Synchrotron. Radiat. **4**, 199 (1997).
[16] E. Gluskin, E. E. Alp, I. McNulty, W. Sturhahn, and J. Sutter, J. Synchrotron. Radiat. **6**, 1065 (1999).
[17] M. Yabashi, K. Tamasaku, S. Kikuta, and T. Ishikawa, Rev. Sci. Instrum. (to be published).
[18] M. Yabashi, T. Mochizuki, H. Yamazaki, S. Goto, H. Ohashi, K. Takeshita, T. Ohata, T. Matsushita, K. Tamasaku, Y. Tanaka, and T. Ishikawa, Nucl. Instrum. Methods Phys. Res., Sect. A **467–468**, 678 (2001).
[19] H. Kitamura, T. Bizen, T. Hara, and X. M. Maréchal, T. Seike, and T. Tanaka, Nucl. Instrum. Methods. Phys. Res., Sect. A **467–468**, 110 (2001).
[20] S. Takahashi, H. Aoyagi, T. Mochizuki, M. Oura, Y. Sakurai, A. Watanabe, and H. Kitamura, Nucl. Instrum. Methods. Phys. Res., Sect. A **467–468**, 758 (2001).
[21] Y. Tanaka, T. Hara, H. Kitamura, and T. Ishikawa, Rev. Sci. Instrum. **71**, 1268 (2000).
[22] T. Ishikawa, Y. Yoda, K. Izumi, C. K. Suzuki, X. W. Zhang, M. Ando, and S. Kikuta, Rev. Sci. Instrum. **63**, 1015 (1992); T. S. Toellner, T. Mooney, S. Shastri, and E. E. Alp, Proc. SPIE Int. Soc. Opt. Eng. **1740**, 218 (1992).
[23] A. Souvorov, Proc. SPIE Int. Soc. Opt. Eng. **3773**, 14 (1999); K. Tamasaku and T. Ishikawa, *ibid.* **3773**, 207 (1999).
[24] Although we observed a slight increase of the energy resolution for a much larger aperture size horizontally [17], the resolution can be regarded as a constant within this range of the slit widths.
[25] R. Coïsson, Appl. Opt. **34**, 904 (1995).
[26] M. Masaki and S. Takano, in Proceedings of the 5th European Workshop on Diagnostics and Beam Instrumentation, ESRF, Grenoble, 2001 (to be published).